INTERNATIONAL JOURNAL FOR NUMERICAL METHODS IN FLUIDS
Int. J. Numer. Meth. Fluids 2003; **43**:231–252 (DOI: 10.1002/fld.600)

Modelling solitons under the hydrostatic and Boussinesq approximations

Chris Daily*,† and Jorg Imberger

Centre for Water Research, Department of Environmental Engineering, University of Western Australia, Australia

SUMMARY

An examination of solitary waves in 3D, time-dependant hydrostatic and Boussinesq numerical models is presented. It is shown that waves in these models will deform and that only the acceleration term in the vertical momentum equation need be included to correct the wave propagation. Modelling of solitary waves propagating near the surface of a small to medium body of water, such as a lake, are used to illustrate the results. The results are also compared with experiments performed by other authors. Then as an improvement, an alternative numerical scheme is used which includes only the vertical acceleration term. Effects of horizontal and vertical diffusion on soliton wave structure is also discussed. Copyright © 2003 John Wiley & Sons, Ltd.

KEY WORDS: soliton; hydrostatic; Boussinesq; Navier–Stokes

1. INTRODUCTION

A significant area of interest for modellers of small to medium bodies of water, such as lakes and estuaries, is the ability of three-dimensional hydrodynamic models to accurately reproduce important wave events. These events can occur at various spatial and temporal scales, ranging from the size of the entire basin down to a few centimeters. Some examples of basin scale waves are topographic: Kelvin, Rossby, Poincaré and seiching (for example see [1] or [2]). Medium size waves often as small as several meters are solitons, bores and higher mode Poincaré waves [3–5] or [6]. At the smallest level there are an abundance of free internal waves, nonlinear effects, detailed aspects of the medium scale waves and mixing due to breaking [4, 6–8]. It has long been proposed that in combination, these waves lead to intermittent turbulence; something the numerical models may not be able to account for if the internal waves are not reproduced correctly.

To study the modelling of waves in three-dimensional hydrodynamic models, one must consider each class of waves in terms of pure wave theory as well as in light of the theoretical foundations of a particular model. It is also important to verify predictions with good

*Correspondence to: C. Daily, Level 1, 111 Harrington Street, Sydney, NSW 2000, Australia.
†E-mail: daily@alumni.princeton.edu

Received 24 September 2001
Revised 19 May 2003

laboratory results. The work presented here consists of an examination into the nature of solitary waves in models which make the hydrostatic and Boussinesq approximations. In particular a class of long non-linear solitary waves known as solitons is discussed.

The approach is to first review some fully non-hydrostatic soliton theory and then consider the hydrostatic and Boussinesq approximations. While the distortion of gravity waves due to the hydrostatic approximation is generally known to be an issue (e.g. Reference [9]) the topic is discussed in detail for solitons specifically. Once the theory understood, we can then compare the resulting set of equations with those used in specific hydrodynamic models. This is followed by modelling of some example waves under various conditions.

In Section 2 the relevant soliton theory is summarized. Section 3 describes a numerical model which will be used to illustrate the results of Section 2. Section 4 compares numerical modelling of solitary waves with experimental results. Section 5 discusses these results in the context of soliton theory. Finally, results of this study are summarized in Section 6.

2. SOLITONS IN A STRATIFIED FLUID

In general, solitary waves can be described by a Korteweg-de Vries (KdV) type equation. A review outlining some variations of these equations is given by Grimshaw [3, 10]. Theory relevant to the particular non-hydrostatic, non-Boussinesq system under consideration is given by Benney or Kao *et al.* [11, 6, 12]. A detailed derivation under the hydrostatic and Boussinesq approximations can be found in Daily [13].

2.1. General solution

Because a single soliton is a two-dimensional phenomenon we can begin with the 2-D non-diffusive Navier–Stokes equations:

$$u_x + w_z = 0 \tag{1}$$

$$\rho_t + u\rho_x + w\rho_z = 0 \tag{2}$$

$$\rho(u_t + uu_x + wu_z) = -p_x \tag{3}$$

$$\rho(w_t + uw_x + ww_z) = -p_z - g\rho \tag{4}$$

where x is the horizontal direction, z is the vertical direction, t is time, u and w are the horizontal and vertical velocities, ρ is the density, p is the pressure and g is gravity.

The physical setup is assumed to be an essentially two layer stratified fluid in a long box with no mean shear. The state variables can then be split into their mean and perturbed parts. Specifically,

$$\rho = \bar{\rho}(z) + \rho'(x, z)$$

$$u = u'(x, z)$$

$$w = w'(x, z)$$

$$p = \bar{p}(z) + p'(x, z)$$

Substituting the separated variables into (1)–(4) yields the non-linear perturbation equations.

$$u'_x + w'_z = 0 \tag{5}$$

$$\rho'_t + w'\bar{\rho}_z + (u'\rho'_x + w'\rho'_z) = 0 \tag{6}$$

$$(\bar{\rho} + \rho')u'_t + (\bar{\rho} + \rho')(u'u'_x + w'u'_z) = -p'_x \tag{7}$$

$$(\bar{\rho} + \rho')w'_t + (\bar{\rho} + \rho')(u'w'_x + w'w'_z) = -(\bar{p} + p')_z - g(\bar{\rho} + \rho') \tag{8}$$

Next, the following non-dimensional variables are introduced

$$x = \lambda\tilde{x}, \quad z = D\tilde{z} \tag{9}$$

$$u' = \varepsilon U\tilde{u}, \quad w' = \varepsilon W\tilde{w} \tag{10}$$

$$\rho' = \varepsilon\rho_o\tilde{\rho}, \quad \bar{\rho} = \rho_o\bar{\rho} \tag{11}$$

$$p' = \varepsilon\rho_o gD\tilde{p}, \quad \bar{p} = \rho_o gD\bar{p} \tag{12}$$

$$t' = \frac{\lambda}{U}\tilde{t} \tag{13}$$

where λ is the characteristic wavelength, D the undisturbed fluid depth and ρ_o a reference density. The small parameter ε is a perturbation constant usually defined as the ratio of characteristic wave amplitude, $\bar{\eta}$, over the total depth, D. The magnitude of vertical velocity is of order $W = (UD)/\lambda$, which is obtained from the continuity equation. For notational simplicity, $\bar{\rho}$ and $\bar{p}$ have been reassigned to represent the non-dimensional values.

Substituting the above scaling relationships into Equations (5)–(8) and taking $U = \sqrt{gD}$ results in the non-dimensional perturbation equations,

$$\tilde{u}_x + \tilde{w}_z = 0 \tag{14}$$

$$\tilde{\rho}_t + \tilde{w}\bar{\rho}_z + \varepsilon(\tilde{u}\tilde{\rho}_x + \tilde{w}\tilde{\rho}_z) = 0 \tag{15}$$

$$(\bar{\rho} + \varepsilon\tilde{\rho})\tilde{u}_t + (\varepsilon\bar{\rho} + \varepsilon^2\tilde{p})(\tilde{u}\tilde{u}_x + \tilde{w}\tilde{u}_z) = -\tilde{p}_x \tag{16}$$

$$\mu^2(\bar{\rho} + \varepsilon\tilde{\rho})\tilde{w}_t + \mu^2(\varepsilon\bar{\rho} + \varepsilon^2\tilde{\rho})(\tilde{w}\tilde{w}_x + \tilde{w}\tilde{w}_z) = -(\bar{p}/\varepsilon + \tilde{p})_z - (\bar{\rho}/\varepsilon + \tilde{\rho}) \tag{17}$$

where the parameter $\mu^2 = D^2/\lambda^2$ has been defined.

The next step is to eliminate the pressure terms by introducing a stream function and taking the z-derivative of (16) and the x-derivative of (17). If the stream function is defined as

$$\tilde{u} = \psi_z, \quad \tilde{w} = -\psi_x \tag{18}$$

then the resulting set of equations are

$$\tilde{\rho}_t - \psi_x\bar{\rho}_z + \varepsilon(\psi_z\tilde{\rho}_x - \psi_x\tilde{\rho}_z) = 0 \tag{19}$$

$$\{(\bar{\rho}+\varepsilon\tilde{\rho})\psi_{zt}+(\varepsilon\bar{\rho}+\varepsilon^2\tilde{\rho})(\psi_z\psi_{xz}-\psi_x\psi_{zz})=-\tilde{p}_x\}_z \tag{20}$$

$$\{\mu^2(\bar{\rho}+\varepsilon\tilde{\rho})(-\psi_{xt})+\mu^2(\varepsilon\bar{\rho}+\varepsilon^2\tilde{\rho})(-\psi_z\psi_{xx}+\psi_x\psi_{xz})=-(\bar{p}/\varepsilon+\tilde{p})_z-(\bar{\rho}/\varepsilon+\tilde{\rho})\}_x \tag{21}$$

When the pressure terms are eliminated and all terms with an order higher than ε or μ^2 are dropped, Equations (19)–(21) become

$$\tilde{\rho}_t-\psi_x\bar{\rho}_z+\varepsilon(\psi_x\tilde{\rho}_x-\psi_x\tilde{\rho}_z)=0 \tag{22}$$

$$(\bar{\rho}\psi_{zt})_z-\tilde{\rho}_x+\varepsilon[\tilde{\rho}\psi_{zt}+\bar{\rho}(\psi_z\psi_{xz}-\psi_x\psi_{zz}]_z+\mu^2\bar{\rho}\psi_{xxt}=0 \tag{23}$$

Because $\bar{\rho}$, μ^2 and ε are known initialization parameters, (22) and (23) give two equations and two unknowns. They can be solved by defining an expansion for ψ and $\tilde{\rho}$ as follows:

$$\psi(x,z,t)=A\phi^{(0,0)}+\varepsilon A^2\phi^{(1,0)}+\mu^2A_{xx}\phi^{(0,1)}+\text{HOT} \tag{24}$$

$$\tilde{\rho}(x,z,t)=A\rho^{(0,0)}+\varepsilon A^2\rho^{(1,0)}+\mu^2A_{xx}\rho^{(0,1)}+\text{HOT} \tag{25}$$

where the superscripts (i,j) refer to the orders of ε and μ^2, respectively, $\phi(z)$ represents a vertical perturbation structure, $\rho(z)$ is a vertical density structure and $A(x,t)$ defines how the structure evolves over the x and time axis. Substitution of (24) and (25) into (22) and (23) yields the following two directly solvable equations for the vertical, time-independent and horizontal, time-dependent components:

$$(\bar{\rho}\phi_z)_z-\frac{\bar{\rho}_z\phi}{c^2}=0 \tag{26}$$

$$A_t+cA_x+\varepsilon rAA_x+\mu^2sA_{xxx}=0 \tag{27}$$

where r and s are coefficients dependent on $\bar{\rho}(z)$ and $\phi(z)$ and obtained by integrating (26) from $z=0$ to 1, and c is the wave speed. Equation (26) is a simple Sturm–Liouville eigenvalue problem and Equation (27) is the well known KdV equation which has a sech^2 solution. Note that the last two terms in (27) contain non-linear and dispersive effects, respectively, while the first two terms describe linear wave propagation. An example solution to the first and second modes of (26) is shown in Figure 1, while the top panel of Figure 2 shows the first mode solution for $\tilde{\rho}(x,z,t=0)$. When no approximations are made, the wave would propagate along the x-axis with no deformation whatsoever. Making the hydrostatic and Boussinesq approximations changes this dramatically.

2.2. *Hydrostatic and Boussinesq approximations*

If the hydrostatic approximation is initially made, we begin with following equations:

$$\begin{aligned} u_x+w_z&=0\\ \rho_t+u\rho_x+w\rho_z&=0\\ \rho(u_t+uu_x+wu_z)&=-p_x\\ 0&=-p_z-g\rho \end{aligned} \tag{28}$$

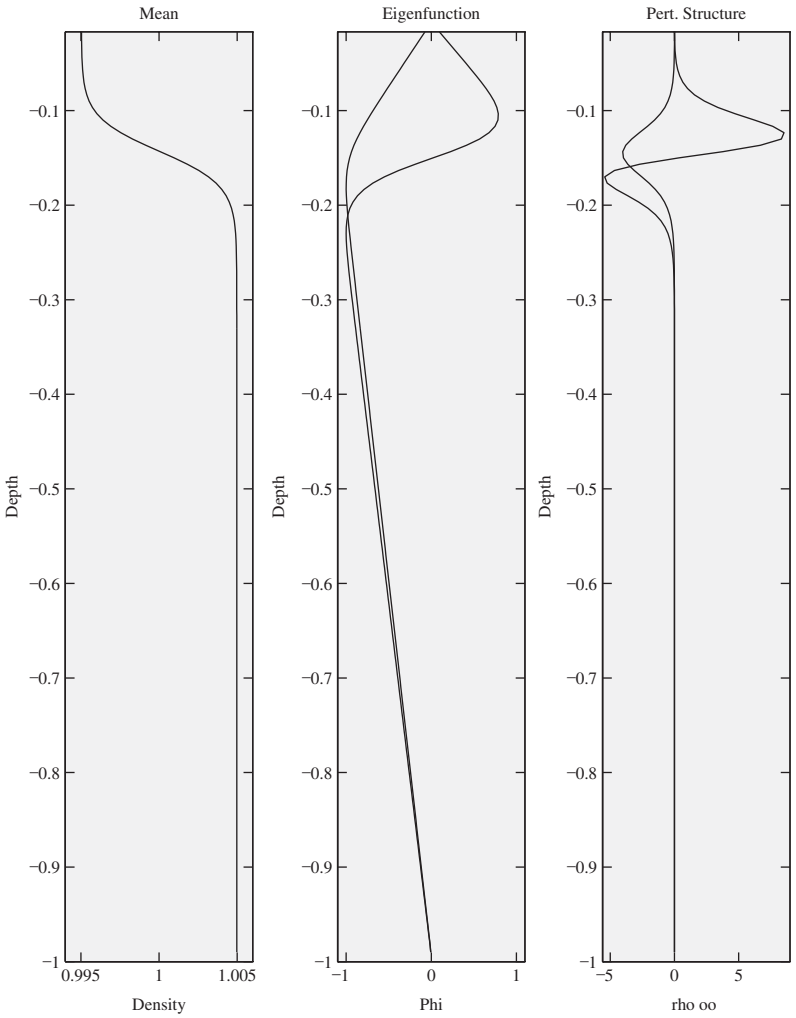

Figure 1. Example initial density profile, corresponding normalized eigenfunctions for the first and second modes, and the resulting density perturbation structure.

Following an identical analysis, it is straightforward to derive the hydrostatic version of Equations (22) and (23):

$$\begin{aligned} \tilde{p}_t - \psi_x \bar{\rho}_z + \varepsilon(\psi_z \tilde{\rho}_x - \psi_x \tilde{\rho}_z) &= 0 \\ (\bar{\rho}\psi_{zt})_z - \tilde{\rho}_x + \varepsilon\,[\tilde{\rho}\psi_{zt} + \bar{\rho}(\psi_z \psi_{xz} - \psi_x \psi_{zz})]_z &= 0 \end{aligned} \tag{29}$$

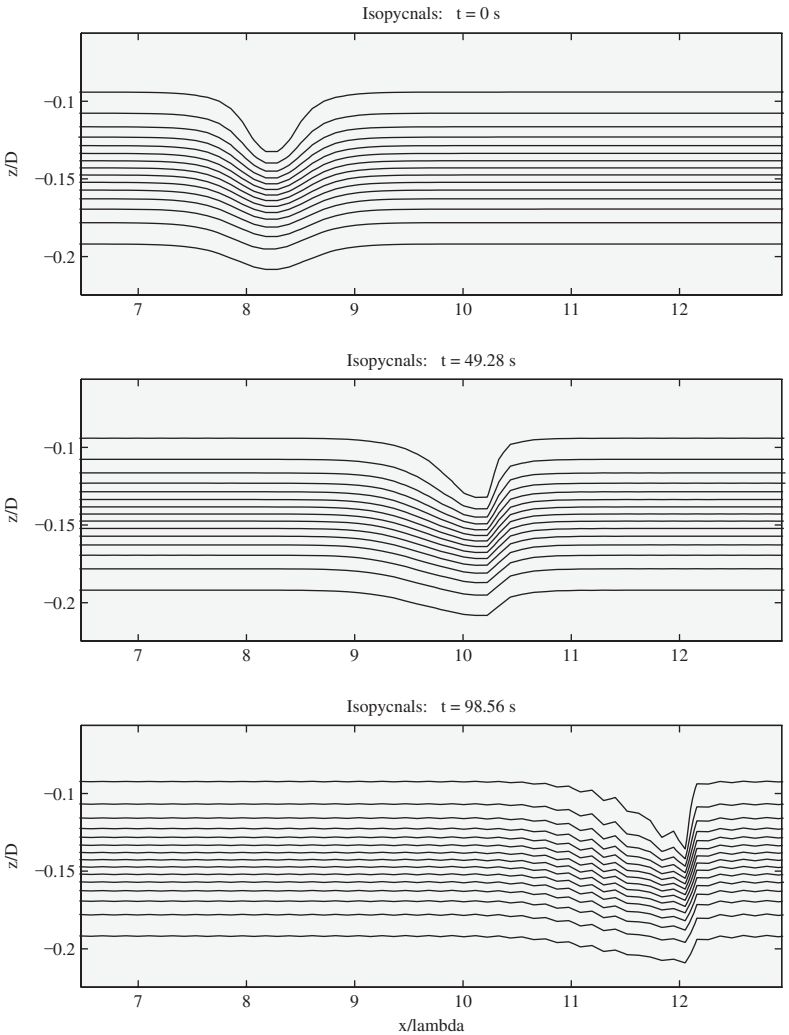

Figure 2. Isotherm displacement for a mode 1 wave. It is the numerical integration of equation 30 using parameters from Table I. Time $t = 0$ (top panel) is a sech^2 displacement which would propagate without changing if the equations were non-hydrostatic. Instead, the wave deforms as it propagates from left to right (middle and bottom panel).

Using a slightly modified expansion for $\psi(x,z,t)$ and $\tilde{\rho}(x,z,t)$, the hydrostatic version of the directly solvable equations becomes

$$\begin{aligned} (\bar{\rho}\phi_z)_z - \frac{\tilde{\rho}_z\phi}{c^2} &= 0 \\ A_t + cA_x + \varepsilon rAA_x &= 0 \end{aligned} \tag{30}$$

Table I. Initial conditions used in the numerical integration of the theoretical hydrostatic propagation equation.

Conditions			
D [m]	$\frac{h_1}{D}$	$\Delta\rho[\frac{\text{kg}}{\text{m}^3}]$	αD
0.356	2/14	10	56
Parameters			
r	$-s/\tilde{c}_o$	c_o [m/s]	
−4.304	0.0231	0.0620	

where c and r are the same as in Equation (27). As expected, the dispersion term $\mu^2 s A_{xxx}$ has dropped out of the horizontal evolution equation. It is well known that the missing dispersion term will cause the wave to steepen as it propagates. Figure 2 illustrates what this looks like for the conditions and parameters listed in Table I.

If instead the Boussinesq approximation is made by setting ρ_o equal to a constant in front of the time-derivative and non-linear terms, we end up with the following series of equations:

$$\begin{gathered} u_x + w_z = 0 \\ \rho_t + u\rho_x + w\rho_z = 0 \\ \rho_o(u_t + uu_x + wu_z) = -p_x \\ \rho_o(w_t + uw_x + ww_z) = -p_z - g\rho \end{gathered} \tag{31}$$

$$\Downarrow$$

$$\tilde{\rho}_t - \psi_x\bar{\rho}_z + \varepsilon(\psi_z\tilde{\rho}_x - \psi_x\tilde{\rho}_z) = 0 \tag{32}$$

$$\rho_o\psi_{zzt} - \tilde{\rho}_x + \varepsilon[\rho_o(\psi_z\psi_{xz} - \psi_x\psi_{zz})]_z + \mu^2\rho_o\psi_{xxt} = 0$$

$$\Downarrow$$

$$(\rho_o\phi_z)_z - \frac{\bar{\rho}_x\phi}{c^2} = 0 \tag{33}$$

$$A_t + c^*A_x + \varepsilon r^*AA_x + \mu^2 s^*A_{xxx} = 0$$

where an asterisk on the constants indicates that the value has been modified by a very small amount compared to the non-Boussinesq theory.

From this overall view, it is clear that each approximation eliminates terms in the actual equations being solved (Equations (22), (23), (29), (32)) and that the resulting simplified evolution equations (26), (27), (30), (33) may or may not be heavily modified. In the hydrostatic case the μ^2 term in (29) is eliminated which in turn eliminates the dispersion term in (30). In the Boussinesq case, however, the $\tilde{\rho}\psi_{zt}$ has been eliminated from (32) and various density coefficients have been made constant, but the resulting evolution equations, (33), have been modified only slightly. As shown in Reference [13], if both approximations are made simultaneously the result is effectively equivalent to that obtained by the hydrostatic approximation.

Perhaps the most important point is that the non-hydrostatic vertical acceleration equations can be linearized without affecting the soliton solution. That is, it is possible to obtain

Equations (26) and (27) without using the full non-hydrostatic Navier–Stokes equations as a starting point. As shown in Reference [13], this is achieved by using $w_t = -p_z - g\rho$ as the evolution equation for vertical velocity. This can easily be implemented in a general numerical model, produces much better results when it comes to soliton propagation, and allows a faster solution than a model which simulates the full Navier–Stokes equations.

3. THE NUMERICAL MODEL

To examine solitons in a numerical model which makes the hydrostatic and Boussinesq approximations, a model was used which is similar to the fixed-grid models described by Casulli and Cheng [14, 15] and Casulli and Stelling [16]. The first two papers describe a fully hydrostatic and Boussinesq model while the third describes how that model can be extended to include the vertical acceleration, non-linear and diffusion terms in its solution. However, since the theoretical analysis presented earlier indicates that some of these terms are not important in soliton propagation, the full scheme of Reference [16] was not implemented. Instead, the hydrostatic model of References [14, 15] was converted to a simplified non-hydrostatic model by including only the time derivative of vertical velocity in the vertical momentum equation. This provides both a tool for validation of the theoretical results, and a scheme which is faster than a fully three-dimensional implementation such as Casulli and Stelling's. Other references which are useful include Reference [17], which only describes the two dimensional model but includes a more complete description of the Eulerian–Lagrangian handling of the explicit terms, References [18, 19] which describe some general Eulerian–Lagrangian topics, and Reference [20] which contains several relevant numerical algorithms.

3.1. Governing equations

Under the Boussinesq approximation, the hydrostatic equations with vertical acceleration take the form

$$\frac{\partial u}{\partial t} + u\frac{\partial u}{\partial x} + v\frac{\partial u}{\partial y} + w\frac{\partial u}{\partial z} - fv = -\frac{1}{\rho_o}\frac{\partial p}{\partial x} + \nu_h\left(\frac{\partial^2 u}{\partial x^2} + \frac{\partial^2 u}{\partial y^2}\right) + \frac{\partial}{\partial z}\left(\nu_v\frac{\partial u}{\partial z}\right) \tag{34}$$

$$\frac{\partial v}{\partial t} + u\frac{\partial v}{\partial x} + v\frac{\partial v}{\partial y} + w\frac{\partial v}{\partial z} + fu = -\frac{1}{\rho_o}\frac{\partial p}{\partial y} + \nu_h\left(\frac{\partial^2 v}{\partial x^2} + \frac{\partial^2 v}{\partial y^2}\right) + \frac{\partial}{\partial z}\left(\nu_v\frac{\partial v}{\partial z}\right) \tag{35}$$

$$\frac{\partial w}{\partial t} = -\frac{1}{\rho_o}\left(\frac{\partial p}{\partial z} + g\rho\right) \tag{36}$$

where $u(x, y, z, t)$, $v(x, y, z, t)$ and $w(x, y, z, t)$ are the x-, y- and z-component velocities, $p(x, y, z, t)$ is the pressure, g the gravity, f the Coriolis parameter, ρ_o a reference density, $\rho(x, y, z, t)$ the density, ν_h the horizontal viscosity constant and ν_v the vertical viscosity constant.

These equations are complemented by the continuity equation

$$\frac{\partial u}{\partial x}+\frac{\partial v}{\partial y}+\frac{\partial w}{\partial z}=0 \tag{37}$$

and the free surface equation

$$\frac{\partial \eta}{\partial t}+\frac{\partial}{\partial x}\left(\int_{-h}^{\eta} u\,\mathrm{d}z\right)+\frac{\partial}{\partial y}\left(\int_{-h}^{\eta} v\,\mathrm{d}z\right)=0 \tag{38}$$

where $-h$ refers to the depth and $\eta(x, y)$ the free surface elevation. The momentum equations are also coupled with the advection diffusion equations for temperature, T, and salinity, S,

$$\frac{\partial c}{\partial t}+u\frac{\partial c}{\partial x}+v\frac{\partial c}{\partial y}+w\frac{\partial c}{\partial z}=v_{ch}\left(\frac{\partial^2 c}{\partial x^2}+\frac{\partial^2 c}{\partial y^2}\right)+\frac{\partial}{\partial z}\left(v_{cv}\frac{\partial c}{\partial z}\right) \tag{39}$$

where c refers to T or S. The equations are closed with the UNESCO equation of state, $\rho=\rho(T,\ S,\ z)$.

In order to separate the hydrostatic solution from the non-hydrostatic solution in these equations, one can assume that the pressure, $p(x, y, z, t)$, may be decomposed into the sum of its hydrostatic and hydrodynamic components, $p_{hs}(x, y, z, t)+p_{hd}(x, y, z, t)$. This allows Equations (34)–(36) to be written as

$$\begin{aligned}&\frac{\partial u}{\partial t}+u\frac{\partial u}{\partial x}+v\frac{\partial u}{\partial y}+w\frac{\partial u}{\partial z}-fv\\&\quad=-\frac{1}{\rho_o}\frac{\partial p_{hs}}{\partial x}-\frac{\partial q}{\partial x}+v_h\left(\frac{\partial^2 u}{\partial x^2}+\frac{\partial^2 u}{\partial y^2}\right)+\frac{\partial}{\partial z}\left(v_v\frac{\partial u}{\partial z}\right)\end{aligned} \tag{40}$$

$$\begin{aligned}&\frac{\partial v}{\partial t}+u\frac{\partial v}{\partial x}+v\frac{\partial v}{\partial y}+w\frac{\partial v}{\partial z}+fu\\&\quad=-\frac{1}{\rho_o}\frac{\partial p_{hs}}{\partial y}-\frac{\partial q}{\partial y}+v_h\left(\frac{\partial^2 v}{\partial x^2}+\frac{\partial^2 v}{\partial y^2}\right)+\frac{\partial}{\partial z}\left(v_v\frac{\partial v}{\partial z}\right)\end{aligned} \tag{41}$$

$$\frac{\partial w}{\partial t}=-\frac{1}{\rho_o}\left(\frac{\partial p_{hs}}{\partial z}+g\rho\right)-\frac{\partial q}{\partial z} \tag{42}$$

where $q(x, y, z, t)$ is the normalized hydrodynamic pressure, p_{hd}/ρ_o. By definition, the hydrostatic pressure gradient in (42) is balanced by the buoyancy term so that we may integrate $\partial p_{hs}/\partial z=-\rho g$ to obtain the following relation for the horizontal gradient of hydrostatic pressure

$$\nabla_h p_{hs}=-g\rho_o\nabla_h\eta-\int_{z^*}^{\eta}\nabla_h\rho'\,\mathrm{d}z^* \tag{43}$$

where the density has been decomposed into its mean and varying parts, $\rho_o + \rho'(x, y, z, t)$. We can now rewrite (40)–(42) as

$$\frac{\partial u}{\partial t} + u\frac{\partial u}{\partial x} + v\frac{\partial u}{\partial y} + w\frac{\partial u}{\partial z} - fv$$
$$= -g\frac{\partial \eta}{\partial x} - \frac{g}{\rho_o}\int_{z^*}^{\eta}\frac{\partial \rho'}{\partial x}\,\mathrm{d}z^* - \frac{\partial q}{\partial x} + \nu_h\left(\frac{\partial^2 u}{\partial x^2} + \frac{\partial^2 u}{\partial y^2}\right) + \frac{\partial}{\partial z}\left(\nu_v\frac{\partial u}{\partial z}\right) \tag{44}$$

$$\frac{\partial v}{\partial t} + u\frac{\partial v}{\partial x} + v\frac{\partial v}{\partial y} + w\frac{\partial v}{\partial z} + fu$$
$$= -g\frac{\partial \eta}{\partial y} - \frac{g}{\rho_o}\int_{z^*}^{\eta}\frac{\partial \rho'}{\partial y}\,\mathrm{d}z^* - \frac{\partial q}{\partial y} + \nu_h\left(\frac{\partial^2 v}{\partial x^2} + \frac{\partial^2 v}{\partial y^2}\right) + \frac{\partial}{\partial z}\left(\nu_v\frac{\partial v}{\partial z}\right) \tag{45}$$

$$\frac{\partial w}{\partial t} = -\frac{\partial q}{\partial z} \tag{46}$$

In general, one can argue that the hydrodynamic gradient terms in (44)–(46) will be relatively small. This is certainly true in situations where the hydrostatic approximation is valid. Furthermore, under the full hydrostatic approximation, the hydrodynamic pressure gradient terms are totally neglected. In that case the resulting equations are those solved by the scheme described in References [14, 15].

3.2. *Numerical scheme*

The approach for solving Equations (44)–(46), in both their hydrostatic and non-hydrostatic forms, is twofold. First, for each time step, the hydrodynamic pressure gradient terms are neglected and the remaining momentum equations solved using the method described in References [15, 14]. This gives an intermediate velocity field which can be used to obtain the final solution. To obtain the hydrostatic solution, the intermediate horizontal velocities are actually the final horizontal velocities and the continuity equation is directly applied to obtain the final vertical velocities.

3.2.1. Non-hydrostatic solution. If the non-hydrostatic solution is desired, the procedure is to reconsider the momentum equations by including the hydrodynamic pressure gradient terms. In discretized form, these are

$$u_{i+1/2,j,k}^{n+1} = \tilde{u}_{i+1/2,j,k}^{n+1} - \frac{\Delta t}{\Delta x}(q_{i+1,j,k}^{n+1} - q_{i,j,k}^{n+1}) \tag{47}$$

$$v_{i,j+1/2,k}^{n+1} = \tilde{v}_{i,j+1/2,k}^{n+1} - \frac{\Delta t}{\Delta y}(q_{i,j+1,k}^{n+1} - q_{i,j,k}^{n+1}) \tag{48}$$

$$w_{i,j,k+1/2}^{n+1} = \tilde{w}_{i,j,k+1/2}^{n+1} - \frac{\Delta t}{\Delta z_{i,j,k+1/2}^{n+1}}(q_{i,j,k+1}^{n+1} - q_{i,j,k}^{n+1}) \tag{49}$$

where the vertical grid spacing as calculated at the intermediate time step, $\Delta z_{i,j,k+1/2}^{n+1}$. Since q is not known at this point, the requirement that the new field be divergence free is used to obtain an equation for q. That is, substituting Equations (47)–(49) into the discretized continuity equation,

$$\begin{aligned} &\frac{u_{i+1/2,j,k}^{n+1}\Delta z_{i+1/2,j,k}^{n+1} - u_{i-1/2,j,k}^{n+1}\Delta z_{i-1/2,j,k}^{n+1}}{\Delta x} \\ &\quad + \frac{v_{i,j+1/2,k}^{n+1}\Delta z_{i,j+1/2,k}^{n+1} - v_{i,j-1/2,k}^{n+1}\Delta z_{i,j-1/2,k}^{n+1}}{\Delta y} \\ &\quad + w_{i,j,k+1/2}^{n+1} - w_{i,j,k-1/2}^{n+1} = 0 \end{aligned} \tag{50}$$

yields

$$\begin{aligned} &\Delta t\left[\frac{(q_{i+1,j,k}^{n+1} - q_{i,j,k}^{n+1})\Delta z_{i+1/2,j,k}^{n+1} - (q_{i,j,k}^{n+1} - q_{i-1,j,k}^{n+1})\Delta z_{i-1/2,j,k}^{n+1}}{\Delta x^2}\right. \\ &\quad \times \frac{(q_{i,j+1,k}^{n+1} - q_{i,j,k}^{n+1})\Delta z_{i,j+1/2,k}^{n+1} - (q_{i,j,k}^{n+1} - q_{i,j-1,k}^{n+1})\Delta z_{i,j-1/2,k}^{n+1}}{\Delta y^2} \\ &\quad \left. + \frac{(q_{i,j,k+1}^{n+1} - q_{i,j,k}^{n+1})}{\Delta z_{i,j,k+1/2}^{n+1}} - \frac{(q_{i,j,k+1}^{n+1} - q_{i,j,k}^{n+1})}{\Delta z_{i,j,k+1/2}^{n+1}}\right] \\ &\quad = \frac{\tilde{u}_{i+1/2,j,k}^{n+1}\Delta z_{i+1/2,j,k}^{n+1} - \tilde{u}_{i-1/2,j,k}^{n+1}\Delta z_{i-1/2,j,k}^{n+1}}{\Delta x} \\ &\quad\quad + \frac{\tilde{v}_{i,j+1/2,k}^{n+1}\Delta z_{i,j+1/2,k}^{n+1} - \tilde{v}_{i,j-1/2,k}^{n+1}\Delta z_{i,j-1/2,k}^{n+1}}{\Delta y} \\ &\quad\quad + \tilde{w}_{i,j,k+1/2}^{n+1} - \tilde{w}_{i,j,k-1/2}^{n+1} \end{aligned} \tag{51}$$

This seven diagonal linear system of $N_xN_yN_z$ equations and $N_xN_yN_z$ unknowns, $q_{i,j,k}^{n+1}$, which is symmetric and positive definite, can be solved using a preconditioned conjugate similar to that outlined in Reference [14]. See Reference [13] for a complete development of the actual procedure used.

In summary, the numerical scheme outlined here provides an elegant method for making comparisons between a purely hydrostatic model and a simplified non-hydrostatic model. While in this implementation only the acceleration term in the vertical momentum equations was added to the hydrostatic model, extending this to a fully three dimensional algorithm is relatively straightforward and the reader can refer to the references for details.

Table II. Parameters for example runs in the both the hydrostatic and non-hydrostatic 3D numerical models.

Case			
(mode 1)	r	s/c	c
$h_1/D = \frac{1}{14}$			
$\alpha D = 56$	−9.0552	−0.0129	0.0242
$h_1/D = \frac{2}{14}$			
$\alpha D = 56$	−4.2952	−0.0235	0.0332
$\alpha D = 28$	−4.1044	−0.0254	0.0321

4. COMPARISONS WITH EXPERIMENTAL RESULTS

To illustrate the conclusions presented in Section 2, the numerical model just described was used to reproduce laboratory experiments of Kao *et al.* [6]. They were able to show that solitons propagating near the surface of a tank satisfy the theoretical predictions of Section 2 (i.e. they demonstrated that Benney's Kdv solution for long nonlinear waves is valid). The basic approach taken here is to take these experimental results and compare them with results of the hydrostatic and non-hydrostatic numerical models.

Three specific initial conditions from Kao *et al.*'s experiments were chosen in order to compare the results with those of the numerical model. Table II summarizes the parameters and associated theoretical coefficients. However, because the results for all three initial conditions lead to the same conclusions about the theory of Section 2 and the numerical model of Section 3, only one set of conditions will be presented in detail: $h_1/D = \frac{2}{14}$, $\alpha D = 56$. Figure 3 shows a cross-section of a soliton propagating under these conditions where the hydrostatic numerical model is being used with no diffusion.

4.1. Hydrostatic model with no diffusion

As can be seen in Figure 3, the system is released on the left hand side from a step like structure. A wave then propagates out to the right. According to theory and experimentation, this wave in a non-hydrostatic model would have a sech^2 distribution in the horizontal direction. However, because the hydrostatic approximation was made in the original model equations, the wave has a steep face and a severely spreading wake.

To make a quantitative comparison with analytical and experimental results, the normalized wave amplitude versus non-dimensional time was plotted. Figure 4 shows results for the hydrostatic model at various locations throughout the tank (0.15 L, 0.35 L, 0.55 L and 0.75 L) for a typical single run. The dashed line shows the analytical sech^2 solution which [6] showed to match their experimental results.

The figure shows that the hydrostatic wave clearly does not match the sech^2 profile. The most obvious feature is that the wave face is too steep. This is of course in agreement with the hydrostatic soliton theory. Also note the effects of the diffusing pycnocline just before the wave face and the severe deformation in the wave tail due to pycnocline spreading.

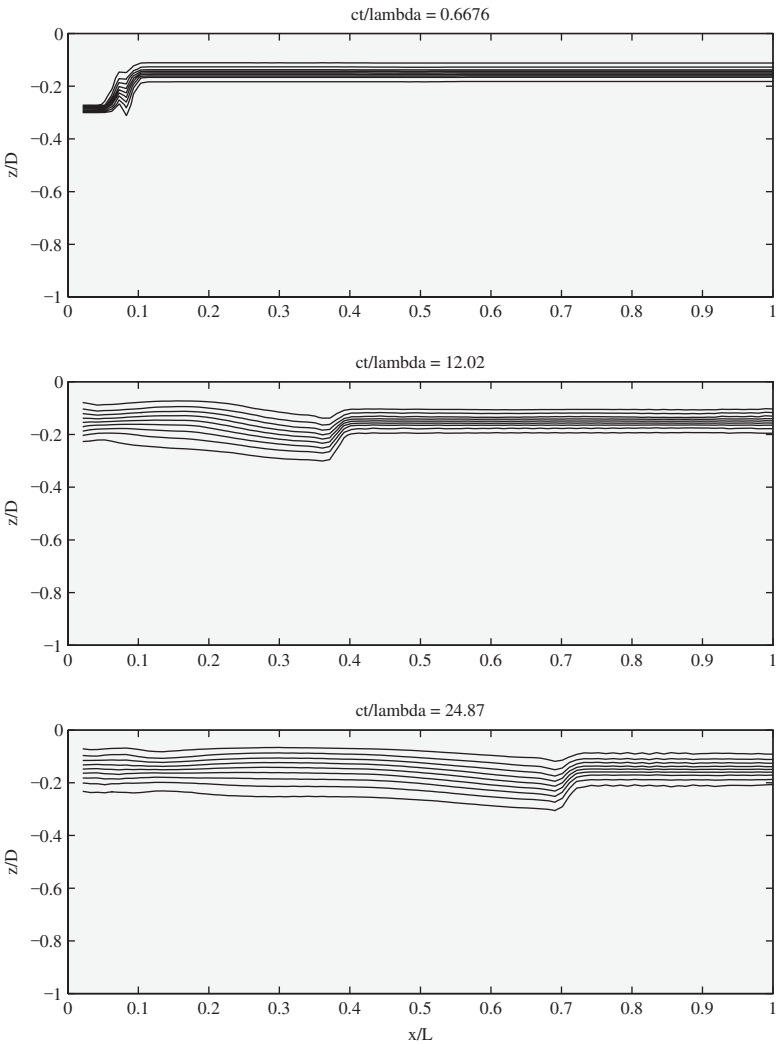

Figure 3. Longitudinal cross-section of an example soliton wave propagating in the 3D hydrostatic numerical model. Both diffusion and viscosity coefficients are set to zero. It is difficult to notice but the wave face is slightly steepened. Also note that there is some pycnocline spreading in the wave wake.

For the positions given above, the series are centred around times of 17.4, 46.2, 73.8 and 102.0 s, respectively. This allows us to calculate an average wave speed of 0.066 m/s, which is faster than the theoretical value of 0.054 m/s for this stratification. All other stratification conditions had wave speeds slightly larger than the theoretical value as well.

From Figure 4 it is seen that in addition to a steepening effect, there is also a decrease in amplitude as the wave propagates further along the tank. Figure 5 illustrates the velocity field and strong gradients at the wave face can be seen. It is likely that these gradients lead to

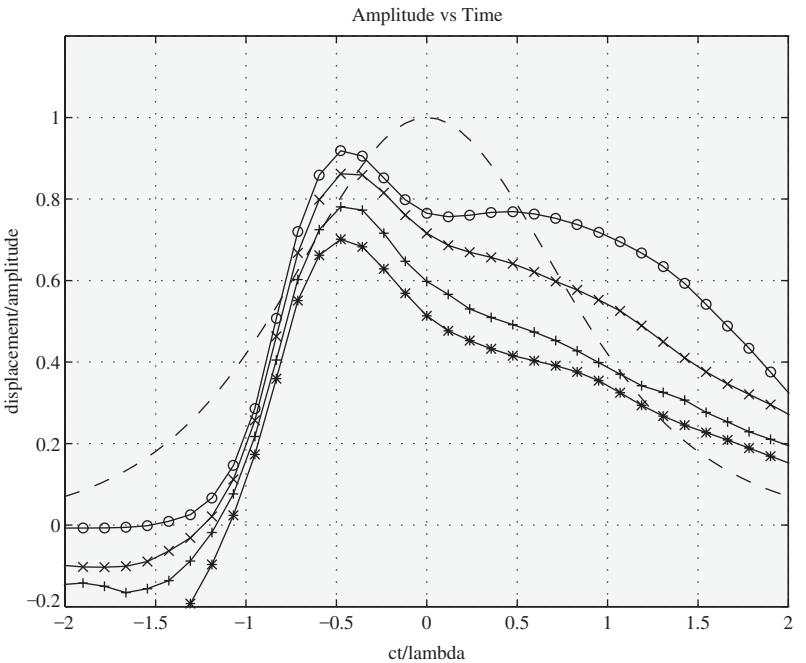

Figure 4. Normalized wave-amplitude vs time (waveform) for a wave in the hydrostatic model. Profiles are at various positions throughout the tank. Each series has been centred so that the effects of propagation on wave amplitude and wavelength can be seen. Diffusion coefficients are set to zero. Positions are at 0.15L (○), 0.35L (×), 0.55L (+) and 0.75L (∗) and centred around times of 17.4, 46.2, 73.8 and 102.0s, respectively. The dashed line represents the analytical solution to the non-hydrostatic, non-Boussinesq equations. Effects of a diffusing pycnocline can be seen just before the wave face. Also, profile is distorted with the wave face being too steep and the tail being too flat.

numerical dissipation (i.e. numerical diffusion of momentum) which can remove energy from the wave motion. Since both the vertical and horizontal diffusion coefficients have been set to zero for this run, any diffusion present is known to be numerical diffusion. It is important to note, however, that without this diffusion the wave would eventually steepen so much that a discontinuity would develop at the face and the model would become unstable. Put another way, for the wave to continue propagating without causing instabilities a balance must occur between the steepening of the wave face and numerical diffusion occurring there due to the strong discontinuities. A similar situation was observed in the numerical integration of the hydrostatic propagation equation (shown in Figure 2). In that case the integration was highly accurate so that numerical diffusion was unable to balance the strong gradient. Eventually the numerical integration became unstable once the wave face reached vertical and hence horizontal derivatives exploded.

4.2. Non-hydrostatic model with no diffusion

Turning our attention toward the non-hydrostatic results, Figures 6 and 7 show the non-hydrostatic equivalent results of Figures 4 and 5. It is immediately seen from Figure 6 that

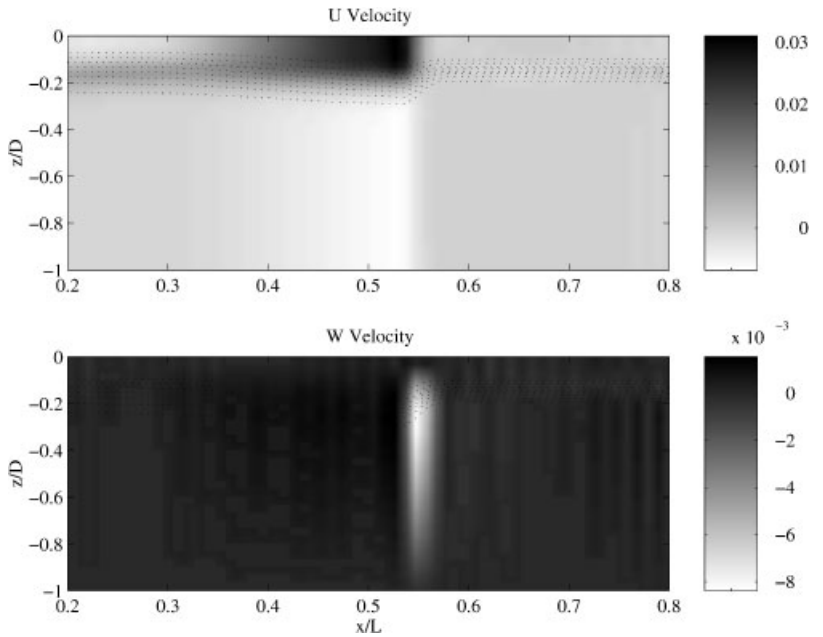

Figure 5. Horizontal and vertical velocities for the hydrostatic model. Dashed lines are the pycnocline contours. Both diffusion and viscosity coefficients are set to zero. Velocities in m/s. Vertical velocity around the wave face is much stronger than at around the tail. Theory predicts a symmetric distribution.

the situation has improved greatly with the addition of the vertical acceleration term. The effects of pycnocline spreading at the wave face have been eliminated and the wave tail is close to its proper sech^2 profile.

It should be noted that in Figure 6, the sampling positions of the time-series had to be adjusted slightly to account for a slower wave speed in the non-hydrostatic model. The new time-series are centred around times of 18.0, 48.0, 76.2 and 105.0 s. This results in an average wave speed of 0.063 m/s, which is an improvement but is still faster than the theoretical value of 0.054 m/s for this stratification.

As for the velocity field, Figure 7 shows that the results have again improved considerably. In the hydrostatic case there was a clear asymmetry about the wave center while in the non-hydrostatic case the velocity fields have become more symmetric. The maximum horizontal velocity magnitude is no longer pushed up near the wave face. Also, the negative vertical velocity field preceding the wave crest has been spread out and there is a much stronger positive vertical velocity following the wave crest. All of these improvements are consistent with the theoretical velocity field.

4.3. Effects of diffusion

Because most of today's 3D numerical models include some sort of closure scheme, often in the form of viscosity and diffusion, it is important to gain an understanding of how adding horizontal or vertical diffusion will affect waves in the numerical models. To this end, the

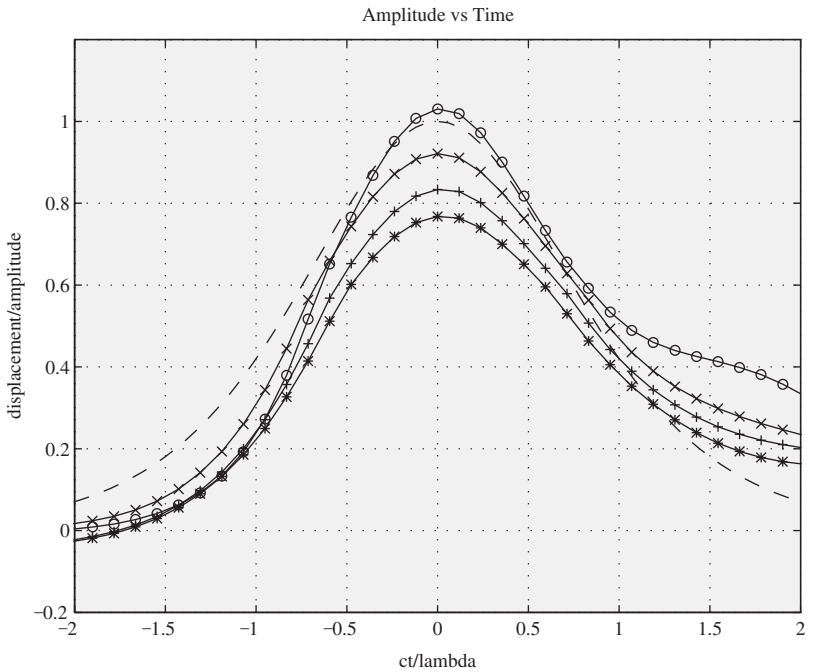

Figure 6. Same as Figure 4 but results are for the non-hydrostatic model. Also, the time-series have been shifted slightly to account for a slightly lower wave speed. Accuracy has improved considerably.

above examples were modified so that horizontal diffusion and viscosity were added without vertical diffusion and viscosity. The runs were then repeated with diffusion and viscosity in the vertical direction, but none in the horizontal direction.

Hydrostatic model with horizontal diffusion. For the horizontal diffusion runs, the diffusion coefficients (v_h and v_{ch}) were set to 3.0×10^{-3} m^2/s and again, vertical coefficients (v_v and v_{cv}) were set to zero. Figure 8(a) shows the wave propagation results. The same non-dimensionalizations as were used in the non-diffusive case have been applied to the amplitude time series (i.e. the analytical values for c and λ were used). The wave speed has been affected very little, but Figure 8(a) illustrates clearly that the wave is always spread out and reduced in magnitude. Furthermore, there is deformation of the wave occurring as it propagates. Initially the wave has a relatively steep front with strong velocity gradients. Because of the gradients the wave face is smoothed by diffusion and energy is dissipated as time progresses. It is tempting to think that this diffusion represents some sort of non-hydrostatic process such as turbulence at the wave face, but we know from theory that the strong velocity gradient needed to trigger such a process should not exist. Hence, we can be reasonably confident that to model the process correctly a non-hydrostatic model should be used.

Non-hydrostatic model with horizontal diffusion. The same initialization and diffusion conditions, but for the non-hydrostatic model are shown in Figure 8(b). It shows that the wave-

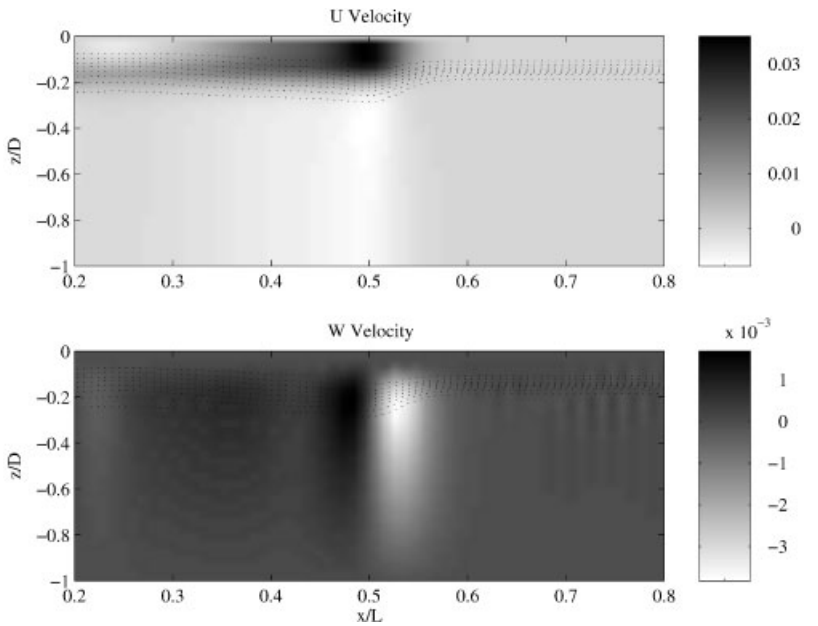

Figure 7. Same as Figure 5 but results are for the non-hydrostatic model. Both the horizontal and vertical velocity fields show a symmetric distribution of velocity which is in good agreement with theory.

form still holds a sech^2 profile, but the wave amplitude is reduced. There is, however, some waveform distortion occurring. This seems to resemble the hydrostatic case (Figure 8(a)) in that the wave starts out steep at the wave face, but slowly smooths out as the wave propagates along the tank. The difference is that for the non-hydrostatic case, the deformation and amplitude reduction are much less severe. This is consistent with our previous view that including the non-hydrostatic process should reduce the velocity gradient at the wave face and therefore make for a more realistic solitary wave.

Hydrostatic model with vertical diffusion. Figure 8(c) shows the hydrostatic model results where horizontal diffusion coefficients are set to zero and vertical coefficients to $5 \times 10^{-5}\,\mathrm{m}^2/\mathrm{s}$. The wave structure has been relatively unaffected by vertical diffusion. It seems plausable that this is because the only place $\partial u/\partial z$ has any significant magnitude is at the base of the wave. That is, at the wave face and tail, the horizontal velocity gradient is dominant, not the vertical gradient. The vertical velocity gradient is important at the base of the wave and should cause mixing there. The true magnitude of this effect is hard to determine though because of the background spreading in the wave wake. On the other hand, it is possible that the velocity shear at the wave base could be the cause of the wake spreading. If this were true, one possible solution might be to go to a higher accuracy scheme for the Eulerian–Lagrangian method since it is well known that low accuracy implementations can cause significant numerical diffusion.

Non-hydrostatic model with vertical diffusion. Results for the non-hydrostatic model with vertical diffusion turned out to be similar to the hydrostatic case. Figure 8(d) illustrates that

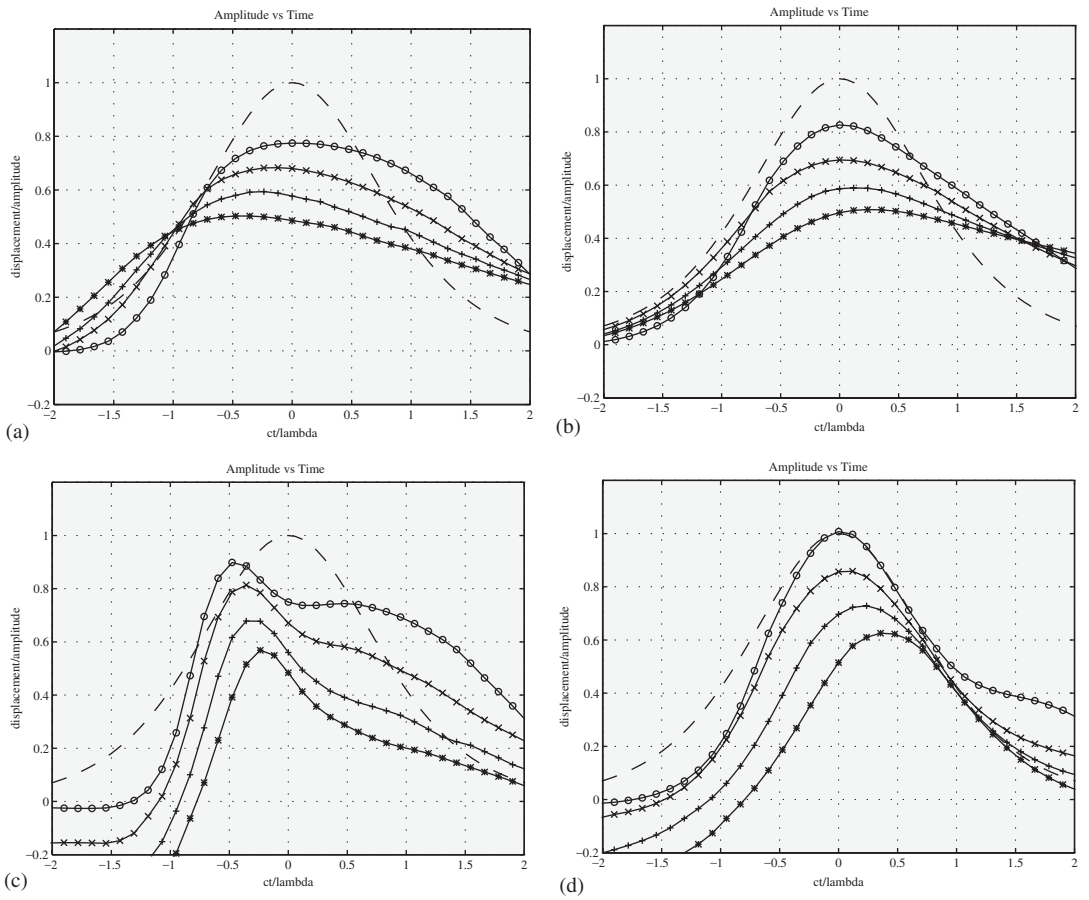

Figure 8. All figures same as Figure 4 but for different model configurations. (a) Results are for the hydrostatic model with horizontal diffusion and viscosity coefficients of $3 \times 10^{-3}\,\mathrm{m}^2/\mathrm{s}$. The waveform now mildly resembles a sech^2 wave but this is due to diffusion at the wave face instead of dispersion. (b) Results are for the non-hydrostatic model with horizontal diffusion and viscosity coefficients of $3 \times 10^{-3}\,\mathrm{m}^2/\mathrm{s}$. Unlike the hydrostatic case, the waveform maintains its original shape but with reduced amplitude. (c) Results are for the hydrostatic model with vertical diffusion and viscosity coefficients of $5 \times 10^{-5}\,\mathrm{m}^2/\mathrm{s}$. This plot clearly demonstrates that both the wave speed and amplitude have been reduced. (d) Results are for the non-hydrostatic model with vertical diffusion and viscosity coefficients of $5 \times 10^{-5}\,\mathrm{m}^2/\mathrm{s}$. As in the hydrostatic case, the wave speed and amplitude have been reduced.

again, the wave maintains its non-diffusive shape but the wave amplitude and speed have been reduced.

5. DISCUSSION

Regardless of how exactly a solitary waveform matches its analytical solution, it is clear that once the wave is generated, the hydrostatic approximation will cause the wave to steepen.

Table III. A summary of the wave propagation results for various model parameters. The horizontal and vertical diffusion (of both momentum and salinity) are represented by v_h and v_c, respectively.

Wave propagation results	
Hydrostatic $v_h = 0,\ v_v = 0$	• Steep wave face • Slightly fast wave speed • Strong $\partial u/\partial x$ at wave face
Non-hydrostatic $v_h = 0,\ v_v = 0$	• Very good waveform match • Improvement in wave speed but still slightly fast • Velocity field symmetrical around wave crest. Good match with theory
Hydrostatic $v_h > 0,\ v_v = 0$	• Extreme diffusion at wave face • Initially resembles a soliton • Strong wave deformation as time progresses • Wave speed unaffected
Non-hydrostatic $v_h > 0,\ v_v = 0$	• Good match • Reduced amplitude • Wave speed unaffected
Hydrostatic $v_h = 0,\ v_v > 0$	• Steep wave face • Reduced amplitude • Reduced wave speed
Non-hydrostatic $v_h = 0,\ v_v > 0$	• Good match • Reduced amplitude • Reduced wave speed

As has been summarized in Table III, this is true for both non-diffusive and diffusive model configurations. The cause of this was clearly seen in Section 2 to be the dropped dispersion term in the evolution equations.

It was also stated in Section 2 that for the full solution, only the vertical acceleration term, w_t in (4), contributes to the actual equations being solved (Equations (22) and (23)). Indeed, when the acceleration term was added to the hydrostatic model, the solitary wave no longer steepened and the wave matched a sech^2 profile very well. The only significant difference between the theoretical wave propagation and modelling result was that the density interface broadened somewhat in the soliton wake. Gross *et al.* [21] have shown that the Eulerian–Lagrangian advection scheme used contains some unavoidable numerical diffusion for these modelling parameters. Thus, as the wave passed along the domain it is likely that numerical diffusion caused the density interface to spread.

5.1. Horizontal diffusion effects

Very few three-dimensional, time-dependent models neglect vertical and horizontal diffusion in the horizontal momentum equations. It is also common to include some sort of closure scheme which modifies the diffusion coefficients such that turbulent mixing is accounted for.

It is important, therefore to understand how addition of horizontal and vertical diffusion will affect the wave propagation results.

When horizontal diffusion of momentum and salinity were included, the results were quite drastic. For the hydrostatic case, the wave was smoothed in the horizontal direction to such an extent that it resembled a sech^2 type wave. However, the wave did not have the correct wavelength, its amplitude decreased rapidly, and its shape deformed as time progressed. In short, it was not a genuine soliton. When acceleration was included in the vertical momentum equation, the wave regained its proper wavelength and shape, but the amplitude still decreased to some degree. It is clear that even in the non-hydrostatic model one must be careful when applying horizontal diffusion.

5.2. Vertical diffusion effects

Inclusion of vertical diffusion proved interesting as well. For both the hydrostatic and non-hydrostatic models the only major effects were reductions in wave amplitude and speed. From the velocity field plots of the non-diffusive runs, it is seen that there is a vertical velocity gradient at the wave base. Since this is the only region where such a gradient exists, it is not surprising that the waveforms remained unchanged. That is, as the wave propagates, the lowering and raising of the wave face and tail does not generate strong vertical velocity gradients in those regions. At the wave base however, there is an evenly distributed vertical velocity shear which gradually diffuses momentum and salinity away from the wave base. The net result is an accentuated pycnocline spreading in the wake and overall reduction in amplitude.

5.3. Improving the numerical scheme

As a final topic, it is worth discussing the computational costs incurred when the previously described scheme is used to include acceleration in the vertical momentum equation. Such a scheme makes the key assumption that the hydrodynamic pressure component will usually be small compared to the hydrostatic component. To obtain a value for this (normalized) hydrodynamic pressure. $q(x, y, z)$, a seven diagonal linear system of $N_x N_y N_z$ equations and $N_x N_y N_z$ unknowns, $q_{i,j,k}^{n+1}$, must be solved, as described in Section 3. Since the computational time required to solve this system of equations at each time step can be equal to or greater than the time required for the entire hydrostatic solution to complete, it is reasonable to consider ways in which this calculation might be improved.

Two possible approaches have appeal. First, because the hydrodynamic pressure field may be localized in certain situations it may be possible to only calculate a local solution where necessary. Figure 9 shows that the magnitude of the hydrodynamic pressure component is fairly localized for solitons. However, it is unlikely that a natural body of water will have only a few localize non-hydrostatic phenomenon occurring. More importantly, q is found by solving an elliptic problem which is by definition non-local. The second possible approach is to only solve for q at periodic intervals rather than at every time step of the main hydrostatic optimization. This would work for processes which had a slowly moving hydrodynamic pressure component. Unfortunately, in the case of solitons the hydrodynamic pressure component moves at the same velocity as the wave. It might be possible to go through few hydrostatic iterations per hydrodynamic iteration, but this method seems ill suited for quickly moving solitons.

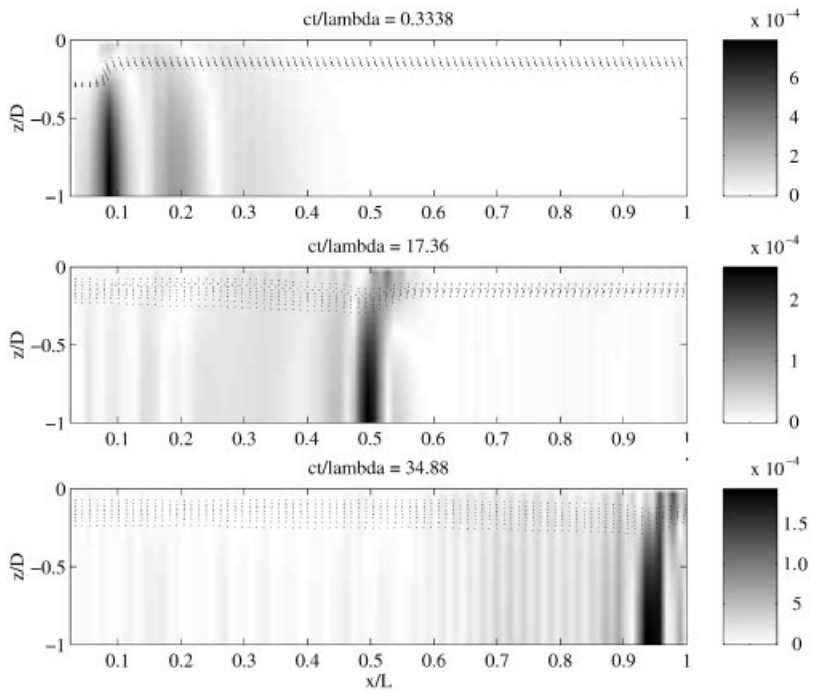

Figure 9. Magnitude of the hydrodynamic pressure component for three time steps. No diffusion or viscosity is used. Note the reasonably localized pressure field. Vertical bands are negligible grid scale inaccuracies which do not show up in the resulting velocity fields.

6. SUMMARY

This study showed that solitary waves cannot be modelled correctly while making the hydrostatic approximation. Inclusion of acceleration in the vertical momentum equation results in a drastic improvement in wave propagation but problems still remain. Specifically, all solitary waves modelled, regardless of the generation mechanism used, caused spreading of the pycnocline as they propagated along. It is most likely that this is due to strong numerical diffusion associated with the Eulerian–Lagrangian method but it also may be a result of inadequate modelling of wave generation caused by neglecting the non-linear terms in the vertical momentum equation.

Results of including diffusion were straightforward. For horizontal diffusion, the hydrostatic waves were severely spread out due to strong horizontal velocity and density gradients at the wave face. They resembled solitons in their form, but the effect is due to mixing rather than pure wave propagation. The only affects on the non-hydrostatic waves was a slight reduction in amplitude.

Vertical diffusion affected both hydrostatic and non-hydrostatic waves such that their amplitude and speed were reduced but their waveform was unaffected. It seems that these reductions must be due to increased diffusion at the base of the wave since that is the only place $\partial u/\partial z$ has a significant magnitude.

Finally, efficiency of the numerical scheme was discussed in the context of localized and/or slowly moving hydrodynamic pressure activity. Proposed solutions to speed up the calculation had potentially serious flaws.

REFERENCES

1. Hutter K. Linear gravity waves, Kelvin waves and Poincaré waves, theoretical modelling and observations. In *Hydrodynamics of Lakes*, Hutter (ed.). Springer Verlag: New York, 1984.
2. Mortimer CH. Lake hydrodynamics. *Mitteilungen Internationale Vereiningung Für Limnologie* 1974; **20**: 124–197.
3. Grimshaw R. Internal solitary waves. *Technical Report*, Monash University, Australia, 1996.
4. Helfrich KR. Internal solitary wave breaking and run-up on a uniform slope. *Journal of Fluid Mechanics* 1992; **243**:133–154.
5. Saggio A, Imberger J. Internal wave weather in a stratified lake. *Limnology and Oceanography* 1998; **43**: 1780–1795.
6. Kao TW, Pan F-S, Renouard D. Internal Solitons on the Pycnocline: Generation, Propagation, and Shoaling and Breaking over a Slope. *Journal of Fluid Mechanics* 1985; **159**:19–53.
7. Horn DA, Imberger J, Ivey GN. The degeneration of basin-scale internal waves in lakes. *Journal of Fluid Mechanics* 2001; **434**:181–207.
8. Uittenbogaard RE, Imberger J. The importance of internal waves for mixing in a stratified estuarine tidal flow. *PhD Thesis*, Delft Hydraulics, 1993.
9. Gill AE. *Atmosphere-Ocean Dynamics*. Academic Press: New York, 1982.
10. Grimshaw R. Evolution equations for long nonlinear waves in stratified shear flows. *Studies in Applied Mathematics* 1981; **65**:159–188.
11. Benney DJ. Long non-linear waves in fluid flows. *Journal of Mathematical Physics* 1966; **45**:52–63.
12. Kao TW, Pao H-P. Wake collapse in the thermocline and internal solitary waves. *Journal of Fluid Mechanics* 1979; **97**(1):115–127.
13. Daily CJ. Numerical modelling of solitary waves under the hydrostatic and Boussinesq approximations. *Masters Thesis*, University of Western Australia, 1999.
14. Casulli V, Cheng RT. Semi-implicit finite difference methods for three-dimensional shallow water flow. *International Journal for Numerical Methods in Fluids* 1992; **15**:629–648.
15. Casulli V, Cheng RT. Stability, accuracy and efficiency of a semi-implicit method for three-dimensional shallow water flow. *Computers and Mathematics with Applications* 1994; **27**(4):99–112.
16. Casulli V, Stelling GS. Simulation of three-dimensional, non-hydrostatic free-surface flows for extuaries and coastal seas. In *Estuarine and Coastal Modelling. Proceedings of the 4th International Conference*, 1995.
17. Casulli V. Semi-implicit finite difference methods for the two-dimensional shallow water equations. *Journal of Computational Physics* 1990; **86**:56–74.
18. Casulli V, Notamicola F. An Eulerian–Lagrangian method for tidal current computation. In *Computer Modelling in Ocean Engineering* Schrefler B, Zienkiewiczoc (ed.). Balkema: Rotterdam, 1988.
19. Cheng RT, Casulli V, Milford SN. Eulerian–Lagrangian solution of the convection–dispersion equation in natural coordinates. *Water Resources Research* 1984; **20**(7):944–952.
20. Greenspan D, Casulli V. *Numerical Analysis for Applied Mathematics*, *Science*, *and Engineering*. Addison Wesley: Reading, MA, 1988.
21. Gross ES, Koseff JR, Monismith SG. An evaluation of advective schemes for estuarine salinity simulations. ASCE *Journal of Hydraulic Engineering* 1999; **125**:32–46.

